

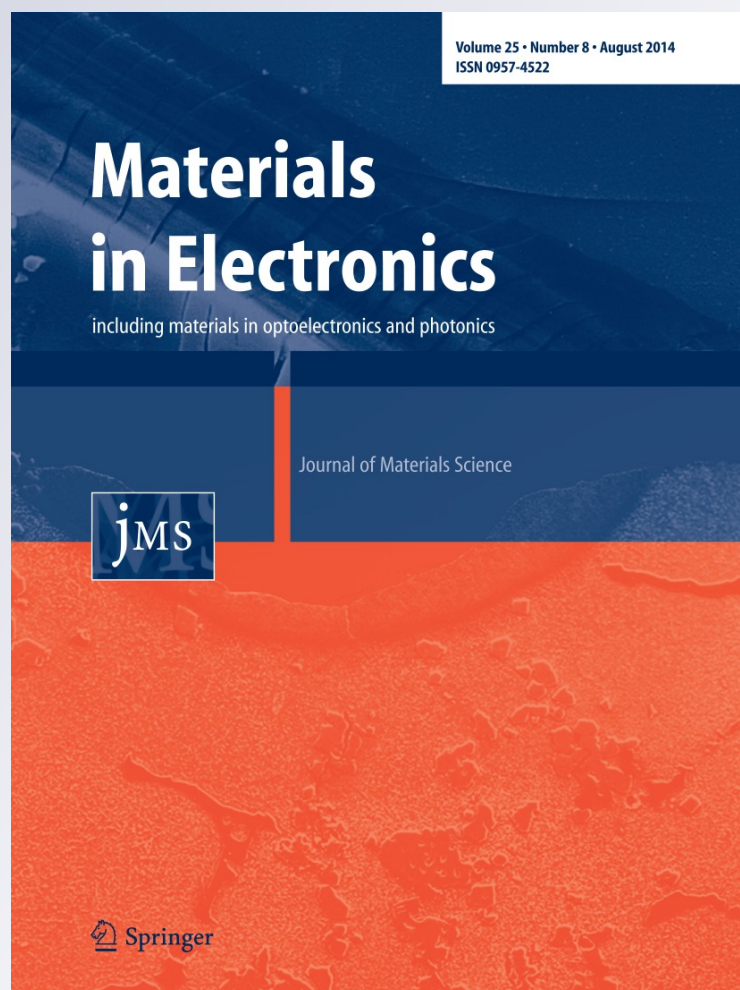
Improvement of the critical current density in Bi-2223 ceramics by sodium–silver co-doping

Berdan Özkurt

**Journal of Materials Science:
Materials in Electronics**

ISSN 0957-4522
Volume 25
Number 8

J Mater Sci: Mater Electron (2014)
25:3295-3300
DOI 10.1007/s10854-014-2017-9



Your article is protected by copyright and all rights are held exclusively by Springer Science +Business Media New York. This e-offprint is for personal use only and shall not be self-archived in electronic repositories. If you wish to self-archive your article, please use the accepted manuscript version for posting on your own website. You may further deposit the accepted manuscript version in any repository, provided it is only made publicly available 12 months after official publication or later and provided acknowledgement is given to the original source of publication and a link is inserted to the published article on Springer's website. The link must be accompanied by the following text: "The final publication is available at link.springer.com".

Improvement of the critical current density in Bi-2223 ceramics by sodium–silver co-doping

Berdan Özkurt

Received: 17 April 2014 / Accepted: 14 May 2014 / Published online: 21 May 2014
© Springer Science+Business Media New York 2014

Abstract $\text{Bi}_{1.46}\text{Pb}_{0.36}\text{Ag}_{0.18}\text{Sr}_2\text{Ca}_3\text{Cu}_{4-x}\text{Na}_x\text{O}_y$ ($x = 0, 0.05, 0.1$ and 0.25) samples were prepared by a conventional solid state reaction method. The prepared samples are characterized using X-ray powder diffraction, scanning electron microscope, dc electrical resistivity and magnetic-hysteresis loop measurements. It has been shown that the Na doping in low contents significantly improves the physical properties of Bi-2223 phase. Magnetic hysteresis measurements have shown that the largest hysteresis curve belongs to $\text{Bi}_{1.46}\text{Pb}_{0.36}\text{Ag}_{0.18}\text{Sr}_2\text{Ca}_3\text{Cu}_{3.95}\text{Na}_{0.05}\text{O}_y$ sample including $x = 0.05$ Na content, indicating that it has best flux pinning capability in samples produced in this work. In addition, J_c values of the samples were calculated from the hysteresis loop measurement by using the Bean's model showing that J_c increases with small amounts of sodium–silver co-doping.

1 Introduction

Many groups have attempted to solve the problems of BSCCO superconductors such as low J_c capacity in applied high magnetic field due to poor flux pinning or weak coupling between grains since their discovery [1]. On the other hand, BSCCO ceramics compared with other HT_c also have important advantages such as their preparations by low cost and being less harmful to human health during the preparation process of the samples.

The favorable studies in order to create the effective pinning centers or increase the hole carrier concentration in the Cu–O planes in BSCCO ceramics have been performed

by doping and adding of many metallic elements such as Na, Ni, Nb, B, Cd, Sn, Ag, Pb [2–15]. It is well known that improvement of J_c in any high superconductors strongly depend on enhancement of the interconnectivity of the grains or introduction new pinning centers into the structure. The magnetic properties of high temperature superconductors can also be enhanced if these doping elements cause a reduction of weak links of the grains.

The mechanical properties of BSCCO system for industrial applications must also be improved. One of the best solutions to improve mechanical properties is that the optimum amount of Ag element enters into BSCCO system [3], since it can improve the links between the grains and the structure of the Bi-based superconductor.

On the other hand, grain properties of BSCCO ceramics strongly affect J_c and H_c values. At applied high magnetic fields, J_c quickly can decrease with the penetration of the magnetic flux into the grains while J_c is high in low magnetic fields. So the structure of grains in HT_c is very important. BSCCO systems generally have randomly oriented plate-like grains. When the grain orientation is smooth and their thickness is wide, enhancements in the hysteresis loops (M – H) is possible, implying higher J_c values according to the Bean model [16]. Many works show that the best current transport and superconducting properties occur when there is a good alignment of the c -axis nearly perpendicular to the growth direction in the grain orientation, which it can be easily done by LFZ technique [17–19]. In addition, some useful alkaline metals such as Li, Na positively affect the grain size of the BSCCO ceramics, presumably due to the reduced phase formation temperature [15, 20]. These results clearly show that when appropriate elements enter into the BSCCO systems, critical current densities (J_c) can be easily increased by enhancing grain structures.

B. Özkurt (✉)

Department of Energy Systems Engineering, Faculty of Tarsus Technology, University of Mersin, Mersin, Turkey
e-mail: berdanozkurt@mersin.edu.tr

In this work, the effects of sodium–silver co-doping on the properties of Bi-based HT_c were investigated. Bi_{1.46}Pb_{0.36}Ag_{0.18}Sr₂Ca₃Cu₄O_y was chosen as the preliminary composition, since it is quite suitable to reach the high production of superconducting phase in the BSCCO system [21, 22]. Samples were synthesized by the conventional solid-state reaction technique. The prepared samples have been characterised using X-ray powder diffraction (XRD), scanning electron microscope (SEM), electrical resistivity and magnetic measurements.

2 Experimental

Bi_{1.46}Pb_{0.36}Ag_{0.18}Sr₂Ca₃Cu_{4-x}Na_xO_{12+δ} ($x = 0, 0.05, 0.1$ and 0.25) polycrystalline samples were prepared from commercial Bi₂O₃ (Aldrich, 99 %), PbO₂ (Aldrich, 99.9 %), Ag₂O (Aldrich, 99 %), SrCO₃ (Alfa Aesar, 99.99 %), CaCO₃ (Aldrich, 99.9 %), CuO (Aldrich, 99.99 %), and Na₂CO₃ (Aldrich, 99 %), powders. Samples were prepared by a conventional solid-state reaction method. They were weighed in the appropriate proportions, mixed and milled. After milling process, the homogenous mixture of powders was pressed into pellets of 1.3 cm diameter by applying a 375 MPa pressure and calcined at 750 °C for 12 h. The calcined pellets were reground, repressed and recalcined twice at 820 °C for 24 h to start the formation of the superconducting phase.

Finally, the precursor materials produced were annealed at 850 °C for 182 h in air to produce the high temperature phase, followed by very slow cooling up to room temperature in the furnace.

The samples with $x = 0, 0.05, 0.1$ and 0.25 will be hereafter named as A, B, C, and D, respectively.

Resistivity and magnetic measurements were carried out on samples using Cryogenic Limited PPMS (from 5 to 300 K) which can reach the cryogenic temperatures about to 2 K a closed-loop He system. X-ray powder diffraction analyses to determine the phases present in the samples were performed by using a Rigaku Ultima IV X-ray diffractometer with a constant scan rate (2 °/min) between $2\theta = 3^\circ$ – 90° . Lattice parameters have been automatically calculated by the PDXL software version 1.6.0.1 with the ICDD version 6.0 database. The surface morphologies of the samples were studied by using a Zeiss/Supra 55 SEM.

3 Results and discussions

3.1 XRD characterization

The powder XRD patterns of all samples are shown in Fig. 1. Each X-ray peak line of the samples is indexed by

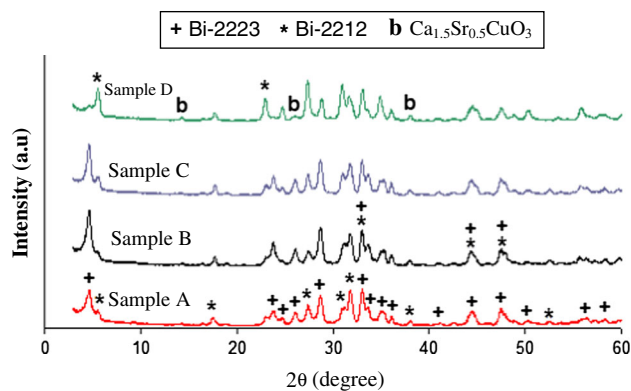


Fig. 1 XRD patterns of the A, B, C and D samples. The symbols indicate the different phases: +Bi-2223; *Bi-2212; ^bCa_{1.5}Sr_{0.5}CuO₃

Table 1 XRD and resistivity measurement results for the samples

Samples	a (Å)	b (Å)	c (Å)	T _C ^{onset} (K)	T _C ^{offset} (K)	R (mΩ cm) at 300 K
A	5.401	5.417	37.055	113	63.8	2.93
B	3.829	3.829	36.76	122	71.9	3.15
C	3.821	3.821	37.033	118	65.6	3.47
D	3.818	3.818	30.78	114	45.5	5.68

various symbols and characters to show different phases. According to this figure, despite 2212 phase together with minor non-superconducting phases such as Ca_{1.5}Sr_{0.5}CuO₃ (shown in Fig. 1b) in samples, it can be seen that 2223 phase is found to be the main phase.

It is obvious that high-temperature Bi-2223 phases decompose in 2212 (low T_c phase) for sample D while other samples protect their high T_c phases.

On the other hand, lattice parameters of samples are important to understand their crystal symmetry. As is clearly seen from Table 1, all Na doped samples have tetragonal structure while sample A has orthorhombic structure. In addition, the automatically obtained lattice c parameter decreases from 37.055 to 30.78 Å for sample A and D, respectively. The decrease in the c parameter of sample D refers to low Bi-2212 phase, as expected.

Also, any impurity phase with Na in all samples was not detected by XRD measurements, indicating that it can incorporate into the crystal structure of Bi-2223 phase.

3.2 Electrical measurements

Figure 2 shows temperature dependence of the resistivity for all samples. All the samples show two-step resistivity transition after their superconducting transition temperature. While high T_c (onset) values in all samples reflect to the Bi-2223 phase, their low T_c (offset) values are due to

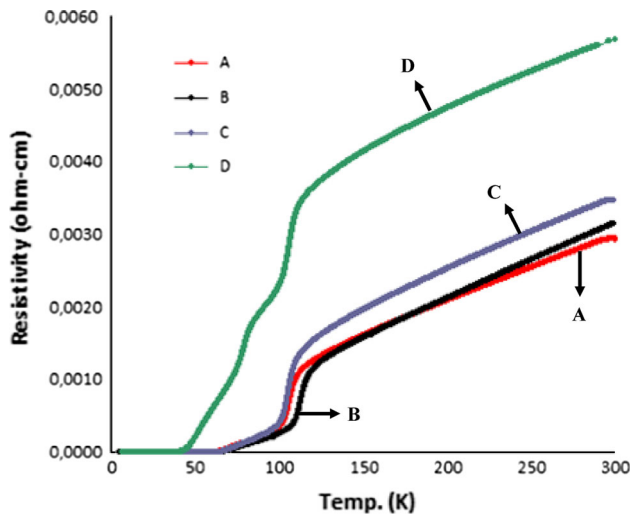


Fig. 2 Resistivity as a function of temperature curves for the samples

parameters such as the intergranular coupling, the presence of impurities or weak links of the superconducting grains [21, 23–26]. The values of the T_c (onset) temperatures observed from the resistivity graph are 113, 122, 118, and 114 K, respectively.

On the other hand, T_c (offset) transition temperatures of the A, B, C, and D samples are found to be about 63.8, 71.9, 65.6, and 45.5 K, respectively. Low T_c (offset) transition temperatures in the samples also show that there are some problems such as insufficient and weak link connections between grains, negative changes in oxygen content due to probably material preparation conditions. Particularly, low T_c (offset) transition temperatures of samples can depend on the used slow cooling after sintering, causing insufficient oxygen content in the samples [27, 28].

Additionally, the transition width ΔT_c ($T_c^{onset} - T_c^{offset}$) obtained from Fig. 2 is the quite wide, implying that there are a combination of both Bi-2212 and Bi-2223 phases instead of desired pure Bi-2223 phase in samples. It is well known from literature that BSCCO system can produce non-superconducting phases due to the controlled decomposition of the superconducting phase when they are exposed to long annealing period at lower temperatures than crystallization temperature to create effective pinning centers [29]. While long annealing period preferred in the preparing of the samples for this work can be useful in many conditions, it looks that this effect destroys the conductivity of grains. The observation of variable value of T_c^{offset} in samples also indicates that the conductivity of grains has different properties and they are strongly affected by the presence of Na. However, the results in this study show that the physical properties of the structure such as T_c (onset) transition temperatures can be improved

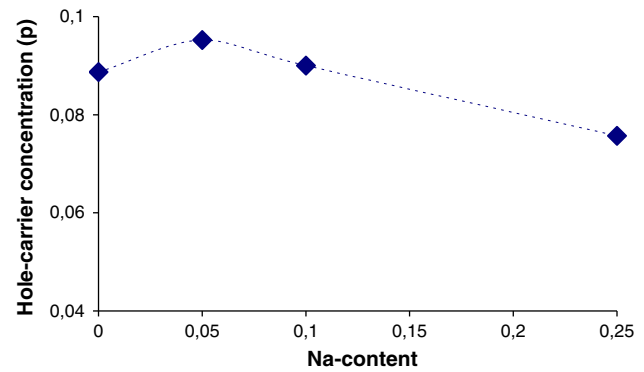


Fig. 3 Variation of hole-carrier concentration versus Na-content

by small amounts of Na doping. Also, samples have a linear temperature dependence on their T_c^{onset} values, indicating that they have metallic characteristics. This behaviour occurs when there are optimally doped carriers in the CuO_2 planes.

3.3 Carrier concentration calculations

The hole-carrier concentrations per Cu ion, P, are calculated by means of the following relation [30]:

$$P = 0.16 - \left[\left(1 - \frac{T_c^{offset}}{T_c^{max}} \right) / 82.6 \right]^{1/2}$$

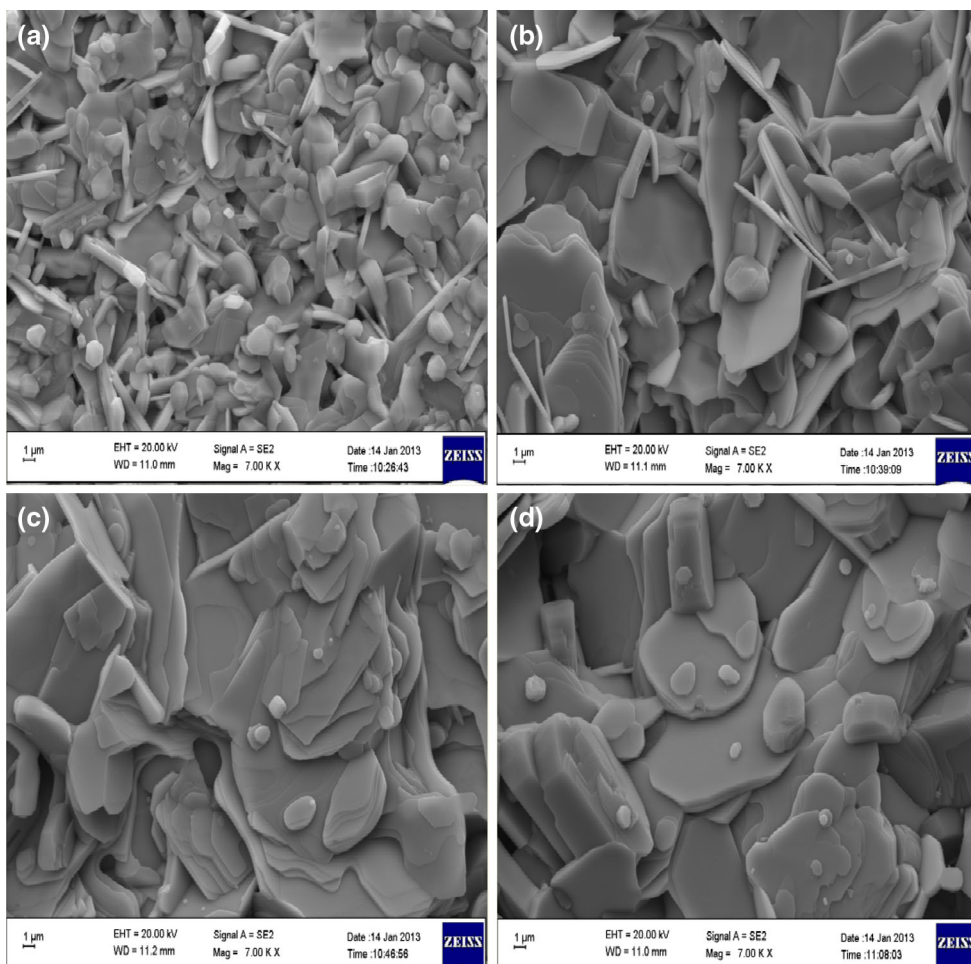
where T_c^{max} is taken as 110 K for Bi-2223 phase [31, 32] and T_c^{offset} values are taken from Table 1. Figure 3 shows the variations of hole-carrier concentrations as a function of Na-content. While an increase in the carrier concentration for sample B and C occurs, sample D has lower carrier concentration due to its low temperature Bi-2212 phase.

Enhancements in hole numbers for sample B and C can be summarized as follows. One would expect that doped metal elements into BSCCO ceramics can prefer to occupy outer Cu sites. When they mainly replace by Cu, they can attract excess oxygen from Bi–O layers which are oxygen poor. Thus, electrostatic forces between charges in Bi–O planes become more stringent, causing a decrease in the length of c axis [33].

On the other hand, as shown in Table 1, there are negligible changes in the c-axis values while a systematic decrease is observed in a and b lattice parameters with the increase of Na content (except sample D), indicating that Na^+ can prefer to incorporate rather than occupation of the Cu sites. Thus, Na had a different ionic radius than that of Cu can cause to degradation bond structures which tends to decrease both a and b axes.

It is well known that the hole carrier density of BSCCO ceramics strongly depends on the average Cu valency. The effective valency of Cu because of the incorporate of Cu^{2+}

Fig. 4 SEM micrographs obtained in the surfaces of **a** $x = 0$, **b** $x = 0.05$, **c** $x = 0.1$, **d** $x = 0.25$ samples



ions by Na^+ ions can increase, implying in a decrease in Cu–O bond length. Note that contractions observed in the a-axis depend on the length of in-plane Cu–O bond [34]. As stated above, increases in the hole concentration is expected with small amount of Na doping.

3.4 SEM analysis

Typical SEM micrographs for all samples are shown in Fig. 4a–d, respectively. One of the important effects on J_c values of BSCCO superconductors is the grain structure which can be positively changed by suitable doping elements or sintering process.

It can be clearly seen from SEM micrographs that the surface morphology of all the samples exhibit granular surface and the large plate-like grains, which are a signature of Bi-2223 phase formation. On the other hand, the plate-like grains in all Na doped samples possess higher sizes than those observed in the undoped A sample. This indicates that the Na doping enhances the formation of high sized grains. Similar results were also observed in the other works doped Na [15] for enhanced granular surface and

bigger plate dimensions. Thus, Na fulfills its task in the structure, which is to create enhancements in size of grains as presumably depending on the reduced phase formation temperature. While sample D also has big grain structure, it shows low T_c (offset) value. Actually, large angle between grains can also create some big porosity while large and smooth grain structure are useful to produce large ΔM (the width of hysteresis loops), destroying grain connectivity and disrupting current flow better. Thus, the increase in the normal state resistivity value along with the long tail in the resistivity of sample D can also be explained by porosity as well as weak intergranular coupling between grains.

3.5 Magnetic properties

The magnetic hysteresis cycles, between applied fields of ± 2 T, for all the samples, at 10 and 25 K, are presented in Figs. 5 and 6, respectively. They demonstrate that increasing Na content causes important changes on the hysteresis width. It is clear that the area enclosed by the magnetization curve increases as the Na content increases up to $x = 0.1$ and then it begins to decrease for higher Na

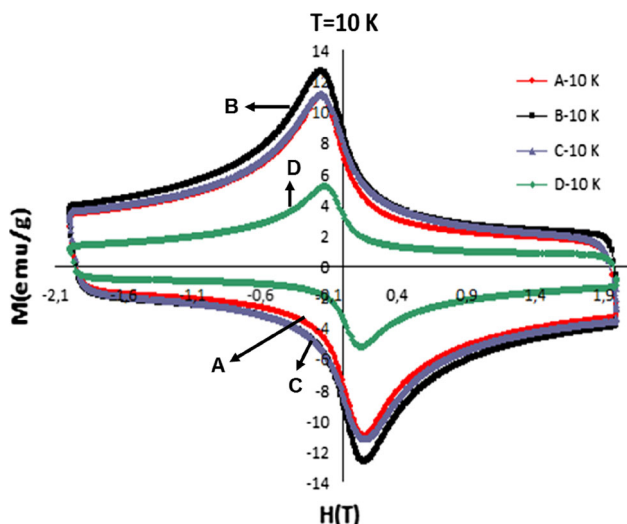


Fig. 5 Magnetization hysteresis curves measured at 10 K

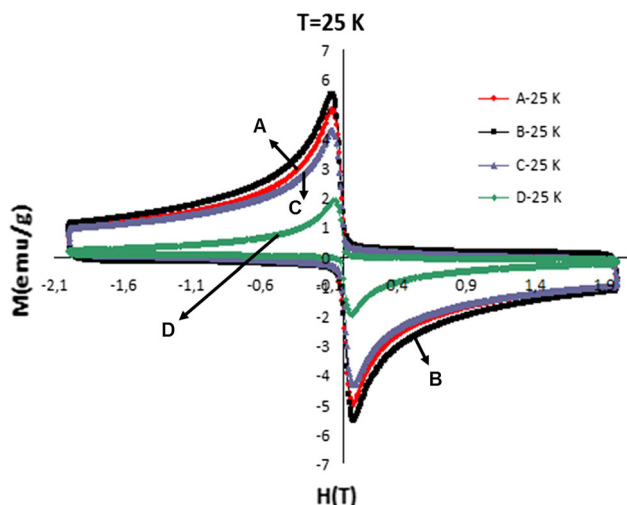


Fig. 6 Magnetization hysteresis curves measured at 25 K

content, such that the width of hysteresis loop significantly decreases for sample D due to its low temperature phase, which can be clearly seen in Fig. 1.

The most important reasons of the decreases in magnetization loops of high temperature superconductors are small coherence length, weak coupling between grains and thermally activated magnetic flux creep. The width of hysteresis loop in ceramic superconductors can be increased by creating pinning centers when appropriate defects or impurities enter into the superconducting matrix. However, enhancements in B and C samples seem to be due to their improving grain structure rather than effective pinning centers. In addition, XRD results show that there isn't any impurity phase with both Ag and Na in all doped samples, implying that they can enter in the Bi-2223

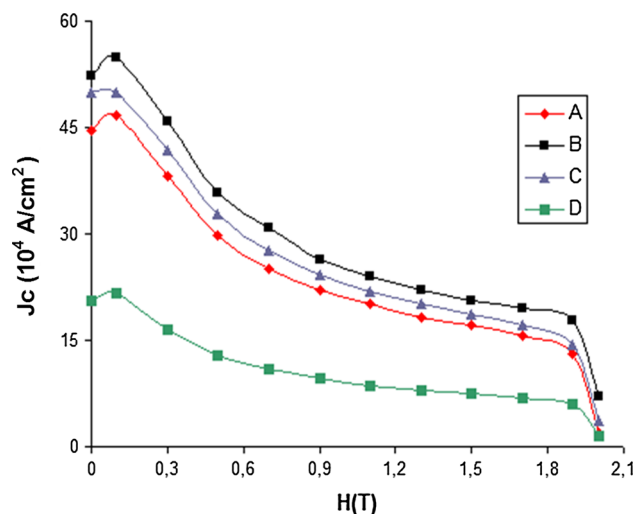


Fig. 7 The calculated critical current densities of the samples at 10 K as a function of applied field

lattice. Enhancement of hysteresis loops in the samples with B and C depends on the increase of diamagnetic response of the Bi-2223 grains, indicating magnetic percolation in the system of Na particles.

The J_c values of the samples were calculated from the hysteresis loops at 10 K, using the Bean's model [35].

$$J_c = 30 \frac{\Delta M}{d}$$

where J_c is the magnetization current density in amperes per square centimeter of a sample. $\Delta M = M_+ - M_-$ is measured in electromagnetic units per cubic centimeter, d is the thickness of sample.

Figure 7 shows the calculated critical current densities for all the samples, as a function of the applied field, at 10 K. As can be seen, the increasing grain size of the samples by increasing the amount of Na causes an increase in the critical current density for sample B.

In addition, SEM results have indicated that grain size of all Na-doped samples is larger than those of undoped sample, implying high J_c values. However, there are a lot of parameters to achieve high J_c values in BSCCO system. It is well known from literature that when the current flows in a conductor, it prefers the lowest resistivity paths. Nevertheless, when we talk about on J_c , we must take into account the area through which the current flows. Thus J_c values strongly depends on not only the current flow path but also many important properties such as the weak coupling and amounts of impurity phases at grain boundaries, the number of grain boundaries and the size and angle of the grains, etc.

Thus, J_c values for sample D quickly decrease with the applied magnetic field due to parameters stated in the previous paragraph although there are improvements in the size and structure of grain with increasing Na content.

4 Conclusions

In conclusion, effects of Na and Ag substitutions on superconductor properties of the BSCCO system have been investigated. The best superconducting behavior in M–H graphics belongs to sample B, which might be due to enhancement of its weak links between grains. Clearly important enhancement in the critical current density (J_c) for sample B shows the effect of grain structure and grain boundaries on magnetic properties of polycrystalline cuprate superconductors.

It was observed that the onset critical transition temperature and remnant magnetization for sample B increased from 113 to 122 K and from 11 to 12.6 emu/g at 10 K, in comparison with those of undoped samples.

Acknowledgments All samples have been prepared in the MEİTAM Central Laboratory in Mersin University in Turkey. SEM measurements have been made in the MEİTAM Central Laboratory in Mersin University, the other measurements in this study have been made in the METU Central Laboratory in Middle East Technical University in Ankara in Turkey. On the other hand, I wish to thank M.Sc. Aynur GÜRBÜZ in the MEİTAM Central Laboratory and M.Sc. Ali GÜZEL, Dr. Ibrahim ÇAM in the METU Central Laboratory for their experimental support and very meticulous work.

References

- H. Maeda, Y. Tanaka, M. Fukutumi, T. Asano, *Jpn. J. Appl. Phys.* **27**(2), L209–L210 (1988)
- H. Sözeri, N. Ghazanfari, H. Özkan, A. Kılıç, *Supercond. Sci. Technol.* **20**, 522 (2007)
- A. Sotelo, M. Mora, M.A. Madre, J.C. Diez, L.A. Angurel, G.F. de la Fuente, *J. Eur. Ceram. Soc.* **25**, 2947 (2005)
- L. Jiang, Y. Sun, X. Wan, K. Wang, G. Xu, X. Chen, K. Ruan, J. Du, *Phys. C* **300**, 61 (1998)
- M. Zargar Shoushtari, S.E. Mousavi Ghahfarokhi, *J. Supercond. Nov. Magn.* **24**, 1505 (2011)
- A.I. Abou-Aly, M.M.H. Abdel Gawad, R. Awad, I. G-Eldeen, *J. Supercond. Nov. Magn.* **24**, 2077 (2011)
- M. Mora, A. Sotelo, H. Amaveda, M.A. Madre, J.C. Diez, L.A. Angurel, G.F. de la Fuente, *Bol. Soc. Esp. Ceram. Vidr.* **44**, 199 (2005)
- S. Şakiroğlu, K. Kocabaş, *J. Supercond. Nov. Magn.* **24**, 1321 (2011)
- S.M. Khalil, *J. Phys. Chem. Solids* **62**, 457 (2001)
- A. Sotelo, M.A. Madre, J.C. Diez, Sh. Rasekh, L.A. Angurel, E. Martinez, *Supercond. Sci. Technol.* **22**, 034012 (2009)
- M.A. Madre, H. Amaveda, M. Mora, A. Sotelo, L.A. Angurel, J.C. Diez, *Bol. Soc. Esp. Ceram.* **47**, 148 (2008)
- Y.L. Chen, R. Stevens, *J. Am. Ceram. Soc.* **75**, 1150 (1992)
- R. Ramesh, S. Green, C. Jiang, Y. Mei, M. Rudee, H. Luo, G. Thomas, *Phys. Rev. B: Condens. Matter* **38**, 7070 (1988)
- B. Özkurt, *J. Alloys Compd.* **579**, 132 (2013)
- B. Özkurt, *J. Mater. Sci.* **24**, 2426 (2013)
- B. Özkurt, *J. Mater. Sci.* **24**, 758 (2013)
- B. Özçelik, B. Özkurt, M.E. Yakıncı, A. Sotelo, M.A. Madre, *J. Supercond. Nov. Magn.* **26**, 873 (2013)
- B. Özkurt, M.A. Madre, A. Sotelo, M.E. Yakıncı, B. Özçelik, *J. Supercond. Nov. Magn.* **25**, 799 (2012)
- B. Özkurt, M.A. Madre, A. Sotelo, M.E. Yakıncı, B. Özçelik, J.C. Diez, *J. Supercond. Nov. Magn.* **26**, 1093 (2013)
- O. Bilgili, Y. Selamet, K. Kocabaş, *J. Supercond. Nov. Magn.* **21**, 439 (2008)
- H. Salamati, P. Kameli, *Phys. C* **403**, 60 (2004)
- S. Kao, K.Y. Simon, *J. Supercond.* **4**, 179 (1991)
- A. Biju, P.M. Sarun, R.P. Aloysius, U. Syamaprasad, *J. Alloys Compd.* **454**, 46 (2008)
- O. Ozturk, E. Asikuzun, M. Erdem, G. Yıldırım, O. Yildiz, C. Terzioğlu, *J. Mater. Sci.: Mater. Electron.* **23**, 511 (2012)
- A. Ianculescu, M. Gartner, B. Despax, V. Bley, Th. Leby, R. Gavrilă, M. Modreanu, *Appl. Surf. Sci.* **253**, 344 (1996)
- G. Yildirim, E. Yuçel, S. Bal, M. Dogruer, A. Varilci, M. Akdogan, C. Terzioğlu, Y. Zalaoglu, *J. Supercond. Nov. Magn.* **25**, 231 (2012)
- F. Jean, G. Collin, M. Andricux, N. Blanchard, J.F. Marruco, *Phys. C* **339**, 269 (2000)
- E. Natividad, L.A. Angurel, J.M. Andres, M.C. Mayoral, *Supercond. Sci. Technol.* **17**, 308 (2004)
- A. Sotelo, M.A. Madre, S. Rasekh, G. Constantinescu, M.A. Torres, J.C. Diez, *J. Supercond. Nov. Magn.* **26**, 985 (2013)
- B.F. Azzouz, A. Mchirgui, B. Yangui, C. Boulesteix, B.M. Salem, *Phys. C* **356**, 83 (2001)
- M.R. Persland, J.L. Tallon, R.G. Buckley, R.S. Liu, N.E. Floer, *Phys. C* **176**, 95 (1991)
- S. Bal, M. Dogruer, G. Yildirim, A. Varilci, C. Terzioğlu, Y. Zalaoglu, *J. Supercond. Nov. Magn.* **25**, 847 (2012)
- M. Okada, *Supercond. Sci. Technol.* **13**, 29 (2000)
- P.M. Sarun, S. Vinu, R. Shabna, A. Biju, U. Syamaprasad, *J. Alloys Compd.* **472**, 13 (2009)
- C.P. Bean, *Phys. Rev. Lett.* **8**, 250 (1962)